Highlights

To cut or not to cut: Effect of vegetation height and bulk density on wildfire propagation under varying wind and slope conditions

Mohammad Tavakol Sadrabadi,Mauro Sebastián Innocente

- Examining wildfire propagation in grasslands combining field-scale simulations and experimental data from the literature
- Cutting grass can curb wildfire propagation and intensity, however, high wind conditions can reverse this effect.
- Identifying bulk density as a key factor for effective wildfire management strategies

To cut or not to cut: Effect of vegetation height and bulk density on wildfire propagation under varying wind and slope conditions

Mohammad Tavakol Sadrabadi, Mauro Sebastián Innocente*

Autonomous Vehicles & Artificial Intelligence Laboratory, Coventry University, 7th Floor Friars House, Manor House Drive, Coventry, CV1 2TE, UK

ARTICLE INFO

Keywords:
Wildfire Propagation
Wildfire Management
Grass Mowing
Fire Dynamics Simulator (FDS)
Fire-Wind Interaction
Very Large-Eddy Simulation
Byram Energy Criterion

ABSTRACT

The frequency, intensity and span of wildfires have surged in the past decades, mainly driven by global changes in climatic patterns. While grasslands cover nearly 40 % of the Earth's surface, they account for approximately 80 % of the burned area caused by wildfires. Aiming to limit the Rate of Spread (RoS) and intensity of grassland fires, mowing is typically adopted as a management strategy in different parts of the world. However, recent studies suggest that the RoS may actually increase when grasses are cut, and therefore this strategy may need reconsideration. This paper combines results from previous experimental studies conducted in Australian grasslands with a significant number of three-dimensional field-scale wildfire propagation simulations under different ambient wind velocities, vegetation heights, and terrain slopes to assess whether *grass cutting* is an effective strategy to mitigate fire propagation in grasslands. Simulations are carried out using the Fire Dynamics Simulator (FDS). Previous investigations on how the vegetation height (H_g) affects the RoS of the fire have led to contradictory results. In this paper, we have found a positive correlation between H_g and $RoS/u_{10}/M$ instead, where RoS/u_{10} is the relative RoS, u_{10} is the wind speed 10 m above ground level, and M is the fuel moisture content. This was observed across all datasets considered and all simulations conducted, provided that the bulk density of the fuel decreases with increasing H_g—as is typically observed in nature—and that the fire is in plume-driven propagation mode. For wind-driven propagation, the reverse is observed in simulations: decreasing H_g (shorter grass, decreasing fuel load, increasing bulk density) leads to increasing RoS/u_{10} for constant M. Further experimental research is needed to confirm this trend, which appears somewhat counter-intuitive. These findings suggest that the practice of mowing grasses can effectively curb fire propagation, although it may be rendered ineffective and even counter-productive under specific conditions such as areas prone to high winds, as both vegetation characteristics and fire propagation modes significantly affect the fire dynamics.

1. Introduction

The complex interactions between biological, climatic, physical, and social factors influence the likelihood of a wildfire ignition, as well as its spread, intensity, duration, and span. Global changes in climate, land use, management techniques, and population are altering wildfire risk in various parts of the world. Areas previously impacted by wildfires might observe changes in risk—whether increasing or decreasing—whereas those that have never had a wildfire before are now at increased risk. Wildfires can potentially devastate roads and other infrastructure, disrupt natural processes such as the supply of water, and cause immediate and long-term adverse effects on public health. In addition, such incidents may interfere with transport and supply chains, leading to road and business closures. Moreover, smoke from wildfires contains hazardous compounds and fine particulates produced by combustion which pose health threats, particularly at the wildland-urban interface (WUI) [45].

Grasslands cover up to 50M km^2 ($\approx$ 37 %) of the Earth's terrestrial surface [37], and comprise more than 80 % of the world's burned land [23]. Grasslands constitute almost 40 % [16] of the land in the United Kingdom (UK), while 70 % of the land is covered by grasslands in Australia [21]. This highlights the importance of studying grassland fires, which differ from forest fires in various ways. For instance, due to their well-aerated structure, the high surface-to-volume ratio of grass litter, and the lack of trees to obstruct the wind, they may have an extremely high Rate of Spread (RoS), hence posing high levels of danger to people and buildings [42]. The RoS of the fire is generally a function of the interplay between topographical, weather, and fuel factors. These include atmospheric conditions such as ambient wind speed, humidity, and temperature; topographic conditions such as slope; and fuel conditions such as vegetation type, height, density, and moisture content [21, 27].

Weather and atmospheric parameters significantly affect the fire propagation dynamics. Wind, specifically ground-level or near-surface wind, is the most studied parameter in fire–atmosphere interaction. Generally, wind accelerates the RoS of the fire by supplying it with fresh oxygen and by tilting the flame towards the fresh, unburned fuel, leading to an increased preheating of the fuel by diffusion and/or radiation, and transferring the hot air through the wet fuels through a convective process. Additionally, the wind moves firebrands over long distances, causing new outbreaks ahead of the main fire front [40]. Various researchers have investigated the relationship between the *fire RoS* and the

*Corresponding author
tavakolsam@uni.coventry.ac.uk (M. Tavakol Sadrabadi); mauro.s.innocente@coventry.ac.uk (M.S. Innocente)
pureportal.coventry.ac.uk/en/persons/mohammad-tavakol-sadrabadi (M. Tavakol Sadrabadi); msinnocente.com/webpages (M.S. Innocente)
ORCID(s): 0000-0002-5938-6310 (M. Tavakol Sadrabadi); 0000-0001-8836-2839 (M.S. Innocente)

wind speed. For example, McArthur [24] investigated the effect of the wind on the spread of surface fire in Australian grasslands, proposing that the RoS is a function of the square of the wind speed for winds of up to 10 m/s. However, increasing the wind speed above 12.5 m/s seems to reverse this effect and decrease the RoS instead. One of the most significant contributions to the topic was made by the Commonwealth Scientific and Industrial Research Organisation (CSIRO). In [6], they conducted a large set of experimental grassland fires and examined the effects of wind velocity, fuel moisture content (FMC), fuel load, and fuel height on the behaviour of grassland line fires.They found that even though wind is the most influential factor, other parameters, such as the length of the ignition line, also significantly contribute to the RoS. They also observed two distinct propagation dynamics including (i) a narrow pointed head fire mostly associated with the updraft from the burned area that restricts the lateral spread due to the lateral inflowing winds, and (ii) a broad parabolic-shaped fire with flanks extending beyond the initial ignition length, which tends to propagate faster than the point fire mechanism. In another study [7], combining data from experimental burns and real wildfires, they proposed a new model for predicting the RoS. They proposed a linear relationship between wind speed and RoS for lower wind speeds (below 5 km/h) and a power-law relationship for stronger winds.

Numerous empirical and mathematical models have been developed to predict wildfire behaviour across vegetation types, relying mainly on experimental data and incorporating the Rothermel model [41] and Albini's fuel models [1]. Simple rules of thumb like assuming the RoS to be 10 % [8] or 20 % [9] of the wind speed 10 m above ground level (AGL) are also widely used. These models mainly aid fire services in predicting wildfire RoS during firefighting operations and comprise the basis for more complex models such as FARSITE [15], which provides spatial fire growth estimations. Instead, physics-based models such as the Fire Dynamics Simulator (FDS) [26] and FireProM-F [17, 18] solve the governing equations to simulate fire behaviour with varying levels of detail. A variety of studies have used these models to study wildfire behaviour. For instance, Morvan et al. [30] studied the effect of fire intensity and wind conditions on the unsteady behaviour of the fire front via two-dimensional (2D) simulations. Analysing temporal variations in fire intensity, they found that plume-dominated flames oscillate more rapidly, exhibiting erratic behaviour that is less predictable than that of wind-driven fires.

The terrain slope's effect on the fire behaviour has also been extensively studied, often in combination with wind speed. Rothermel [41] developed a mathematical model that describes the relationship between fire RoS with mid-flame height wind speed and terrain slope. The model quantifies additional propagating flux produced by wind and slope by defining wind and slope coefficients: ϕ_w and ϕ_s, respectively. These coefficients contribute to the overall RoS by being combined with the RoS in flat and windless conditions (RoS_0) as follows: $RoS = RoS_0\ (1 + \phi_\mathrm{w} + \phi_\mathrm{s})$. Weise et al. [47] found that increasing wind speed increases both RoS and flame length. They also validated existing mathematical models against experimental data, and concluded that the existing formulations of empirical fire spread models are inaccurate and need to be revised. Wu et al. [48] studied the interaction of a pool-fire plume with the terrain slope under no-wind conditions, observing that flame bends toward the surface and attaches to the bed as the terrain slope increases. They concluded that this is mainly due to the asymmetric formation of the plumes on either side of the flame. Morandini et al. [29] studied the fire spread dynamics uphill under no-wind conditions using particle image velocimetry and video imaging. They observed that, on horizontal surfaces with radiation as the dominant preheating mechanism, the fire plume maintains a quasi-vertical shape due to the lateral air flow into the fire from either side. By increasing the terrain slope, a strong convective flow forms ahead of the flame due to the pressure difference upstream and downstream of the flame that blows towards the top of the surface contributing to the fuel preheating. Monroy et al. [44] studied the effect of the fuel depth and packing ratio on the fire propagation dynamics at different uphill angles using numerical simulations. Consistently with other studies, they identified a critical slope angle of approximately 22° beyond which rapid increase of the RoS occurs with increasing slope.

Although most studies on upslope fire propagation focus on no-wind conditions, a few have examined the combined effects of wind and slope. Pimont et al. [39] examined the integrated effect of wind and slope on fire RoS, emphasising the impact of fire width using the HIGRAD-FIRETEC model. Their results indicate a significant interaction between wind and slope so that, under low-wind conditions, the RoS increases exponentially with slope until the latter reaches 40 %. Instead, the RoS and slope are linearly related under high-wind conditions. Guo et al. [20] experimentally examined the effects of slope (0°–30°) and wind (0–2 m/s) on surface fire spread over a pine needle fuel bed. Their results indicate that the RoS, flame length, and heat flux increase with increasing wind speed and slope, whilst the flame angle decreases. Additionally, they concluded that the RoS increases linearly with slope for low wind speeds $u < 0.5$ m/s and slopes of up to 30°. However, the RoS accelerates abruptly for higher wind speeds as the slope exceeds 25°, constituting an example of extreme and eruptive wildfire behaviour.

The fuel characteristics's effect on the fire dynamics is controversial, as the literature reports contrasting results. Results from CSIRO experiments [6] indicate that, even though fuel load and vegetation species do not significantly affect fire spread, fires in natural undisturbed vegetation burn approximately 18 % faster than those in cut or grazed ones. Moinuddin et al. [27] utilised FDS to study the effect of relative humidity and fuel moisture content (FMC) on grass fire dynamics. They concluded that reduced humidity and FMC increase RoS and burn intensity, with potential shifts in fire propagation modes. Our study only focuses on vegetation height and bulk density. Cruz et al. [14] conducted 58 experimental fires to study the effect of fuel load on fire behaviour in Australian grasslands. They reported that contrary to the community's common assumptions, a negative correlation between the fuel load and fuel height with the RoS of fire is observed when fuel load is not a limiting factor. In a related study, Moinuddin et al. [28] investigated the effect of fuel height on the fire RoS considering different heights of up to 0.6 m. They concluded that increasing the grass height while keeping a constant bulk density reduces the fire RoS but increases its Intensity (I) and Heat Release Rate (HRR), also shifting the fire propagation mode from wind-driven to plume-dominated. However, Cruz et al. [12] later studied the effect of fuel characteristics on the fire RoS in wheat farms by carrying out 45 experimental burns, finding a positive correlation between vegetation height and RoS, where unharvested grass yielded the fastest RoS and longest flames. Commenting on the findings in [14, 28], Cruz et al. [13] stated that the proposed conclusions are counter-intuitive, as robust empirical evidence supports the positive correlation between fuel height and fire RoS. They reanalysed the data from [6, 12] and stated that the positive correlation of fire RoS with vegetation height is not a matter of debate, arguing that variations in vegetation structure may explain why some studies like [14] fail to observe this relationship. In response to these comments, Sutherland et al. [43] reanalysed the data in [12] combined with a series of numerical simulations (with constant ρ_b) and stated that, below a certain grass height ($\approx$ 0.2–0.24 m), RoS increases with height, which is consistent with [6, 12], where most fires were wind-driven. However, for taller grasses where fires are typically plume-dominated, the RoS decreases with increasing grass height (negative correlation).

Thus, the effect of grass height on fire RoS is still an open question. Previous studies have reported conflicting results, whilst numerical studies rely on simulations with a constant bulk density—which is not the case in natural vegetation. This becomes even more complicated on sloped terrains, where the combined effect of terrain slope, wind conditions, and vegetation height can lead to unexpected results, which have not yet been adequately studied in the literature. Consequently, this paper attempts to address this gap by performing a series of numerical simulations and combining the results with two contradictory experimental studies to investigate the effect of vegetation height and structure on fire propagation dynamics for different terrain slopes and ambient wind speeds. A total of 84 field scale simulations are conducted, and the results are analysed and discussed with regards to the effect of each parameter on the fire RoS and propagation modes.

The remainder of this paper is organised as follows: Section 2 provides an overview of the fire propagation model used in this research (Section 2.1), the reference case and fuel definitions (Section 2.3), the turbulent wind model (Section 2.4), the model gridding (Section 2.5), and the model reliability (Section 2.6); Section 3 presents the results of simulations, including the fire RoS under different wind (Section 3.1) and terrain (Section 3.2) conditions, and the characterisation of the effect of vegetation height and bulk density on the fire dynamics; Section 4 provides a discussion of the results, including an attempt to answer the question of whether *grass cutting* is an adequate management strategy to curb the propagation of the fire; whilst Section 5 provides a summary of the research findings and derived conclusions.

2. Modeling procedure

2.1. Fire dynamics simulator

The Fire Dynamics Simulator (FDS) numerically solves a version of the Navier-Stokes equations adapted to low-speed and thermally-driven flows, emphasising the simulation of smoke and heat transmission from flames. The core algorithm uses an explicit predictor-corrector technique with second-order accuracy in both space and time. Large Eddy Simulation (LES) is used to model turbulence within the solution domain. However, for sufficiently fine meshes, Direct Numerical Simulation (DNS) can be employed as an alternative. FDS typically employs a one-step, mixing-controlled chemical reaction model involving three bundled species: *products*, *fuel*, and *air*. Under certain circumstances, reactions that are not always mixing-controlled and multiple reactions might be taken into consideration. A Cartesian grid is used to discretise the domain and estimate the governing equations [25]. FDS offers different models for stimulating wildfire spread depending on the level of physical details required and the computational resources available: the Lagrangian Particle Model (LPM), the Boundary Fuel Model (BFM), and the Level-Set (LS) model.

2.1.1. *Level set model*

This model is used when wildfires spread across wide regions and the domain cannot be discretised with a grid sufficiently fine for physics-based models. FDS with the Level Set model (FDS-LS) uses the same elliptical spread model as FARSITE, which is based on Huygens' principle for wave-front propagation modelling. It also adopts Rothermel-Albini's RoS formula and Albini's 13 fuel models [25].

2.1.2. *Boundary fuel model*

This model may be used when a coarse grid is desired to discretise a thin layer of vegetation. Here, the vegetation is represented as a porous barrier made up of a layer of wetness, air, and dry vegetation. For grid sizes up to 10 m, the vegetation height can be used although it is not resolved on the grid [25, 46]. In this model, the convective heat transfer is represented by a source term in the one-dimensional heat conduction equation. This equation is applied to both the vegetation layer and the solid ground. Additionally, the transfer of thermal radiation through the vegetation layer is modelled using a one-dimensional radiative transport equation designed for semi-transparent solids. Even though this model might be efficiently utilised in a variety of studies and simulations, our preliminary results indicate that the LPM provides better and more realistic results. Consequently, this study utilises the LPM for the simulations.

2.1.3. *Lagrangian particle model*

In this model, a group of Lagrangian particles heated by convection-radiation heat transfer represents the vegetation. These particles may be grass, trees, leaves, or anything else. LPM may be used to replicate the front, rear, and flank fire across the surface and high-level vegetation (e.g. trees) with appropriate grid refinement [46]. The drag force per unit volume ($\mathbf{f}_b$) exerted by the vegetation is modelled as follows:

$$\mathbf{f}_b = \frac{\rho}{2} C_d \, C_s \, \beta \sigma \mathbf{u} \|\mathbf{u}\| \tag{1}$$

where ρ is the air density, C_d is the drag coefficient defined through laboratory experiments, C_s is the shape factor with the default value of 0.25, β is the packing ratio of vegetation calculated as mass per unit volume divided by material density, σ is the surface-area-to-volume ratio, and $\mathbf{u}$ is the wind velocity.

2.2. Dimensional analysis

Performing dimensional analysis using the Buckingham-pi theorem, Morvan et al. [31] stated that the propagation of fire in grasslands is governed by six parameters, including RoS, wind speed (u_w), load of water and dry fuel inside combustible layer, and the two opposing forces (buoyancy and inertia) that affect the trajectory of flame and plume, represented by the energy rate released by the fire (p_f) and the energy rate of the wind (p_w) defined as follows:

$$p_f = \frac{gI}{c_p T_0} \tag{2}$$

$$p_w = \frac{1}{2} \rho \left(u_w - RoS\right)^3 \tag{3}$$

where I represents fire intensity, $\rho = 1.225$ kg/m^3 is the air density, $c_p = 1010$ J/kg/K is the specific heat capacity, and T_0 is the ambient temperature in Kelvin. By applying the Pi-theorem, they concluded that the problem could be described by three non-dimensional parameters: RoS/u_w), Byram's convective number (N_c), and the fuel moisture content (M), which are related as follows:

$$\frac{RoS}{u_w} = F(N_c, M) \tag{4}$$

where

$$N_c = \frac{2gI}{\rho c_p T_0 \left(u_w - RoS\right)^3} \tag{5}$$

Fire intensity $I = W \times H \times RoS$ (kW/m), W (kg/m^2) is the fuel load, and H (kJ/kg) is the heat of combustion of the fuel. Nelson [34] suggested that for values of $N_c < 2$, the propagation of fire is mainly dominated by the convective heat transfer between the flame and the unburned vegetation ahead of it: the wind-driven fire propagation mode. Instead, $N_c > 10$ leads to a different fire propagation mode, characterised by a vertical visible plume that is mostly governed by buoyancy forces and radiative heat transfer between fuel and flame. Consequently, $2 < N_c < 10$ may be considered a transitory state of fire. While u_w is often used interchangeably with both u_2 and u_{10} in the literature when calculating N_c, this study uses u_{10} in all calculations for consistency.

Table 1
Measured properties of CSIRO C064 and F19 experiments [6, 26].

Property	Unit	Case C064	Case F19
Wind speed (u_2)	m/s	4.6	4.8
Ambient Temperature (T)	°C	32	34
Surface Area to Volume Ratio (σ)	m^{-1}	9,770	12,240
Grass Height (H_g)	m	0.21	0.51
Bulk Mass Per Unit Area (ρ_b)	kg m^{-2}	0.283	0.313
Moisture Fraction (M)	%	6.3	5.8
Measured RoS	m s^{-1}	1.2	1.5

2.3. Reference Case and Fuel Modelling

Numerical simulations are validated against the field scale grass fire propagation experiments carried out in the Commonwealth Scientific and Industrial Research Organisation (CSIRO) fields during July and August 1986 with constant high daily temperatures [6, 7]. During the experiments, air temperature, relative humidity, and solar radiation were measured 1.4 m above ground level (AGL), while wind velocity was measured 2 m AGL. Fuel load and height were sampled at 16 points for each experiment and averaged for each plot. Other fuel characteristics, including surface-area-to-volume ratio and the fuel moisture content (FMC), were measured and recorded for each experiment.

Measured properties of two experiments from [6] are provided in Table 1. The C064 experiment was carried out in a 100 × 100 m^2 field covered with dry Kerosene grass of 0.21 m high, while the F19 experiment was carried out in a 200 × 200 m^2 field covered with dry Kangaroo grass of 0.51 m high. Two workers ignited fires, starting at the midpoint and moving towards the sides of the plot. The length of ignition was 50 m for the C064 and 175 m for the F19 experiments. The fire behaviour and RoS were studied using data gathered from ground observations and oblique aerial photographs.

Following [32], the solid phase thermal degradation of the vegetation is modelled utilising a three-step reaction process including (i) endothermic moisture evaporation, (ii) endothermic pyrolysis of dry vegetation, and (iii) exothermic char oxidation. Thus, the rate of change of the total mass in terms of density of composite solid is calculated as:

$$\frac{\partial \rho_s}{\partial t} = -r_{H_2O} - \left(1 - \nu_{char}\right) r_{pyr} - \left(1 - \nu_{ash}\right) r_{char} \tag{6}$$

where the reaction rates for evaporation of H_2O, pyrolysis of the dry vegetation, and surface oxidation of char as

Table 2
Summary of fuel physical properties and thermal decomposition coefficients.

Property	Unit	$Veg_1(Veg_2)$	Reference
Area to Volume Ratio (σ)	m^{-1}	9,770 (12,240)	[6]
Bulk density (ρ_b)	$kg.m^{-3}$	1.313 (0.616)	[6]
Fuel	-	Cellulose	[46]
Fuel Density (ρ)	$kg.m^{-3}$	512	[46]
Moisture content (M)	%	6.3	[6]
Specific Heat	$kJ\ kg^{-1}\ K^{-1}$	2.1	[3]
Conductivity	$kJ\ kg^{-1}\ K^{-1}$	0.1	[46]
Heat of Evaporation (H_{H_2O})	$kJ\ kg^{-1}$	2259	[2]
Heat of Combustion (H_c)	$kJ\ kg^{-1}$	17,400	[25]
Heat of Pyrolysis (H_{pyr})	$kJ\ kg^{-1}$	418	[2]
A_{pyr}	s^{-1}	1040	[19]
E_{pyr}	$J.mol^{-1}$	61041	[19]
Char Yield (v_{char})	$kg\ kg^{-1}$	0.25	[25]
A_{char}	$kg.m^{-2}.s^{-1}$	465	[4]
E_{char}	$J.mol^{-1}$	68000	[4]
Ash Yield (v_{ash})	$kg\ kg^{-1}$	0.04	[25]
Obukhov Length (L)	m	−500	[46]
Roughness Length(z_0)	m	0.03	[46]
Drag Coefficient (c_d)	-	2.8	[25]
Soil Specific Heat	$kJ\ kg^{-1}\ K^{-1}$	2.0	[46]
Soil Conductivity	$W\ m^{-1}\ K^{-1}$	0.25	[46]
Soil Density	$kg\ m^{-3}$	1,300	[46]
Relative Humidity	%	40	[46]

a function of component densities of composite solid are calculated via Arrhenius kinetics:

$$r_{H_2O} = \rho_{s,H_2O}\ A_{H_2O}\ T^{-\frac{1}{2}} e^{\left(-\frac{E_{H_2O}}{R\,T}\right)} \tag{7}$$

$$r_{pyr} = \rho_{s,dry}\ A_{pyr}\ e^{\left(-\frac{E_{pyr}}{R\,T}\right)} \tag{8}$$

$$r_{char} = Y_{O_2,surf}\ \sigma\ A_{char}\ e^{\left(-\frac{E_{char}}{R\,T}\right)} \tag{9}$$

where σ is the surface area-to-volume ratio of the vegetation, $Y_{O_2,\,surf}$ is the oxygen mass fraction at the material surface, A and E (J/mol) are the pre-exponential factors and activation energy, $R = 8.314$ J/mol/K is the universal gas constant, and T is the absolute temperature in Kelvin [25]. This approach allows for the possibility of parallel drying and pyrolysis, with series char oxidation taking place as char is being produced during pyrolysis [32]. Kinetic constants must be determined for this model, and as the data required for particular fuels is sometimes unavailable—including the vegetations in CSIRO experiments—the kinetic constants of Fir determined by Grishin [19] are used for the pyrolysis model in this study. Table 2 presents the details of the pyrolysis constants, as well as the soil and two vegetation models utilised in this study.

2.4. Turbulent wind model and boundary conditions

FDS offers four options for defining the inlet wind into the domain, including (i) a specified wind speed and direction that remains constant with height, (ii) the Monin-Obukhov similarity theory, (iii) advanced meteorological concepts such as a Geostrophic wind for modelling huge spatial domains, and (iv) the power law approximation or the "wall of wind" model. The latter is widely used due to its simplicity, mainly with a power of 1/7 [26, 21, 28]. However, this model has limitations, as the power value varies with height, surface roughness, and stability conditions [38]. The 1/7 exponent approximates a neutrally stable atmospheric stratification. Notably, the CSIRO C064 experiments were carried out during summer daytimes under consistently warm and dry conditions ($T_{C064} = 32°C$) [6], resulting in an unstable stratification of the atmosphere characterised by convective uprising of warm surface air [36]. Thus, the *Monin-Obukhov* similarity theory, which estimates the vertical wind and temperature profiles based on surface and atmospheric conditions [25], would probably provide a more accurate representation. This theory assumes that wind speed (u) and potential temperature (θ) change with height as follows [25]:

$$u(z) = \frac{u_*}{k}\left[\ln\left(\frac{z}{z_0}\right) - \Psi_m\left(\frac{z}{L}\right)\right] \tag{10}$$

$$\theta(z) = \theta_0 + \frac{\theta_*}{k}\left[\ln\left(\frac{z}{z_0}\right) - \Psi_h\left(\frac{z}{L}\right)\right] \tag{11}$$

where u_* is the friction velocity, $k = 0.41$ is the von Karman constant, z_0 is the aerodynamic roughness length, θ_* is the scaling potential temperature, θ_0 is the ground level temperature, L is the Obukhov length, and Ψ_h and Ψ_m represent similarity functions. A negative value of L (m) determines an unstable stratified atmosphere where the buoyancy-generated turbulence causes large fluctuations in wind velocity and direction and enhances mixing. Based on the suggestions in [46], this study determines an Obukhov length of $L = -500$ m and a roughness length of $z_0 = 0.03$ m.

Turbulence within the domain is simulated utilising the very large eddy simulation (VLES) model, incorporating Deardorff's sub-grid scale (SGS) model to handle turbulent eddy viscosity closure terms. The Van Driest damping model is applied to model the Reynolds stresses in near-wall regions. To replicate the turbulent nature of natural atmospheric winds which significantly impact their behaviour at domain boundaries, this study employs the synthetic eddy method (SEM) [22]. This introduces random eddies into the domain, as in [21, 33]. Given that an accurate representation of the eddy characteristics requires measurements of the turbulent Reynolds stress within the ambient wind and canopy height (see [33]), which are not available here, an arbitrary turbulence intensity of 10% is determined (see [21]). It should be noted that the wind field is allowed to develop throughout the simulation domain for 80 s before igniting the fire. Boundary Conditions include a no-slip condition for the ground surface, with 'open' boundary conditions applied to the rest of the boundaries.

2.5. Simulation domain and gridding

The burnable field simulated in this study includes a vegetation field of 200×200 m^2, allowing sufficient time and space for the fire to reach quasi-steady state, particularly under steep upslope and tall vegetation conditions. Preliminary experiments indicated that increasing domain height beyond 40 m does not affect simulation results. Additionally, in order to eliminate the effects of upwind and downwind boundaries on the fire propagation, a minimum buffer of 150 m was set on both sides. Consequently, the simulation domain of this study, as shown in Fig. 1, is a cuboid measuring 600 m in length, 320 m in width, and 60 m in height.

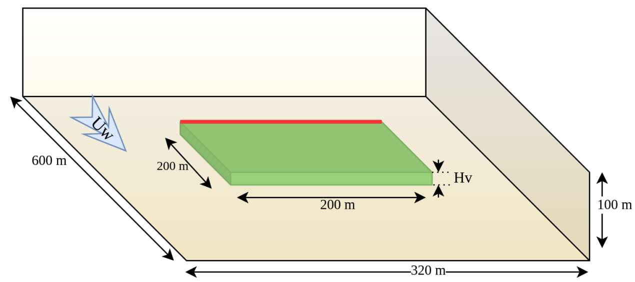

Figure 1: Model Domain

A grid sensitivity analysis was performed to assess the sensitivity of the estimated RoS of the fire to the grid size. Three different grid resolutions of $1 \times 1 \times 1$ m^3 (coarse), $0.5 \times 0.5 \times 0.5$ m^3 (fine), and $0.25 \times 0.25 \times 0.25$ m^3 (very fine) were tested. Results are presented in Fig. 2a, which show a sensitivity to grid size ranging from 6% to 11% across different configurations of wind, vegetation height, and terrain slope. However, despite the benefits in accuracy, the use of the very fine grid is restricted by practical considerations such as the computational requirements (memory, processing) due to the large vegetation area.

Thus, a $0.5 \times 0.5 \times 0.5$ m^3 grid is used for the vegetation domain and its immediate surrounding (±4 m) up to a height of 44 m. Upstream and downstream areas of the fine grid up to a distance of ±30 m are discretised using a 1×1×1 m^3 grid, while the rest of the domain is discretised using a 2×2×1 m^3 grid up to a height of 60 m. A total of 16, 687, 680 grid cells are used, parallelised on 32 CPU cores.

2.6. Model reliability and simulation scenarios

To examine the effect of the turbulence model on simulation accuracy and computational efficiency, three variants are compared: (i) LES, (ii) VLES, and (iii) simple VLES (SVLES). They offer different levels of physical detail and accuracy. Fig. 2 provides the estimated RoS and the heat release rate (HRR) of the combustion for all grid sizes and turbulence models. Fig. 2a compares the fire front location in the C064 experiment with estimations provided by three grid sizes, 1×1×1 m^3 (coarse), 0.5×0.5×0.5 m^3 (fine), and $0.25 \times 0.25 \times 0.25$ m^3 (very fine), and two vegetation types.

The model shows grid dependence for both vegetation types, with RoS decreasing as grid size decreases to 0.25 m. Further reduction in grid size did not affect the RoS. However, the fine grid size is adopted for the main simulations in this study to balance accuracy and computational cost for the large number of simulations carried out. Results show agreement with the experimental measurements. Fig. 2b shows the front location in the C064 experiment for the first vegetation model (Fir) and different turbulence models. Both LES and SVLES predict higher RoS than VLES, in agreement with the experimental results. The HRR for different grid sizes and turbulence models is depicted in Fig. 2c. Like RoS, it is sensitive to the grid size and turbulence model, though the variation is mostly limited to a maximum of 10 % for grid sizes of 0.25 m and 0.5 m. Measured and simulated wind fields at field corners and 2 m AGL are provided in Fig. 2d, showing agreement.

Comparing the simulated and measured fire contours on the x–y plane for the CSIRO C064 experiment (not shown here), it is worth mentioning that, even though the simulated front location aligns with experimental data, the width and flanks of the fire front are less accurately estimated. This is mainly due to the smaller size of the flank flames compared to the front flames, requiring a finer grid to capture their dynamics accurately. To mitigate this and minimise the effect of the length of the ignition line on the estimated RoS, it is kept the same as the width of the field (200 m) for all simulations. It is important to keep in mind that atmospheric conditions such as wind velocity vary rapidly over time in field experiments, affecting fire propagation dynamics. These cannot be reproduced accurately in simulations, which are carried out under more uniform and controlled conditions. Differences between measurements and model predictions are partially due to this.

A total of 84 simulations are performed, with 75 of them using the Veg_1 and the remaining nine using the Veg_2 vegetation models. Three vegetation heights (0.2 m, 0.5 m, 1 m), various terrain slopes $S \in [-21.8°, 21.8°]$, and a range of wind speeds $u_{10} \in [4, 12]$ m/s are considered in the simulations. A summary of the simulated scenarios is provided in Table 3. Note that Veg_2 is only simulated on flat terrain to limit the total number of simulations.

3. Results and analysis

3.1. RoS as a function of wind speed

The RoS is inherently dynamic and oscillatory, which is problematic for comparing different situations. Hence, a quasi-steady RoS is calculated for each scenario, which represents the average value. The quasi-steady RoS is considered to be the slope of the linear regression function fitted to the fire front locations. However, determining the fire front location can be challenging. Therefore, the fire front location at each time instance is identified as the front point along the centerline of the field where the temperature exceeds 400°C measured 25 cm AGL. This height is chosen to minimise the pulsating effect of the flames on the measurements.

Fig. 3 shows the calculated quasi-steady RoS as a function of the wind speed (u_{10}) for different terrain slopes (S) and for three vegetation heights (H_g). Generally speaking, it can be observed that higher wind speed leads to higher RoS regardless of the vegetation height and the bulk density. This increase mostly follows a linear trend, where the fuel with

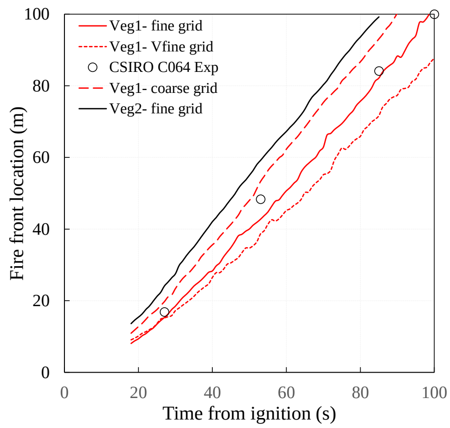

(a) Effect of grid size on fire front location compared to experimental data.

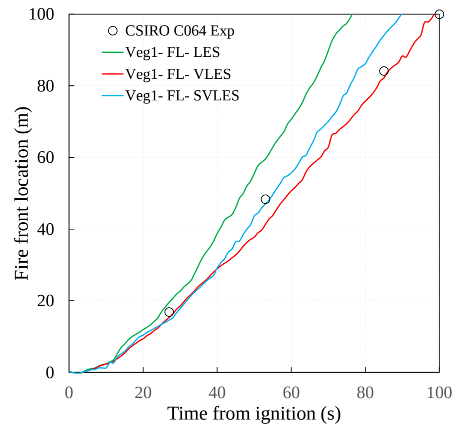

(b) Effect of turbulence model on fire front location.

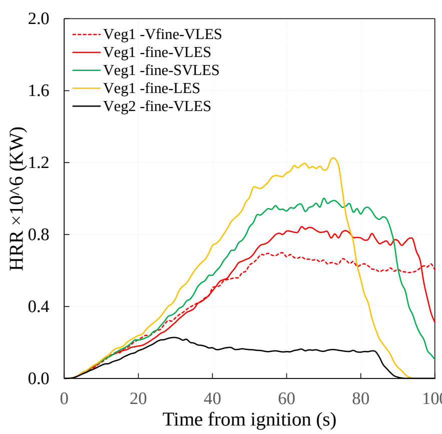

(c) Effect of grid size and turbulence model on obtained HRR.

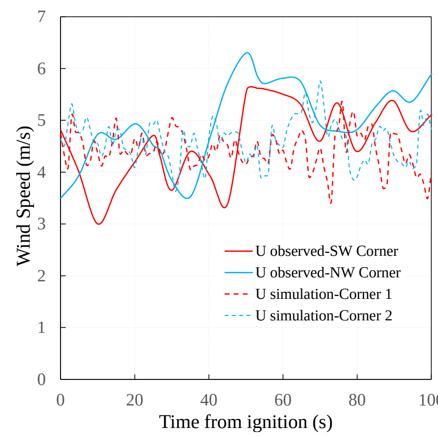

(d) Comparison of measured and simulated wind speed during the experiment.

Figure 2: Model sensitivity and validation analysis.

Table 3
Overview of the simulated geometric and physical properties of the vegetation, terrain, and wind

Vegetation model	Vegetation height (m)	Terrain slope (S)	Wind speed (m/s)	no. simulations
Veg_1	0.2, 0.5, 10	−40 % (−21.8°), −20 % (−11.31°), 0 % (0°), 20 % (11.31°), 40 % (21.8°)	4, 6, 8, 10, 12	75
Veg_2	0.2, 0.5, 10	0 % (0°)	4, 8, 12	9

lower bulk density (Veg_2) results in higher RoS than the fuel with higher bulk density (Veg_1) on horizontal terrain, except for very high wind speeds $u_{10} > 10$ m/s.

Considering the combined effect of bulk density and wind speed, the RoS is observed to be higher at moderate wind speeds (4–8 m/s) for fuels with lower bulk density, regardless of vegetation height. However, it becomes higher for fuels with higher bulk density at $u_{10} > 10$ m/s.

For Veg_1 (constant bulk density), it can be observed that the RoS for shorter grass ($H_g = 0.2$ m) tends to be higher than that for taller grasses ($H_g = 0.5$ m and $H_g = 1$ m), with the RoS decreasing for increasing grass heights. This is consistent with the results in [28]. Under high wind speeds $u_{10} > 10$ m/s and steep slope conditions, the combined effects of vegetation height and terrain can be reversed, resulting in a higher RoS for taller grass ($H_g = 1$ m), even with constant bulk density (see Figs. 3b and 3c).

Fig. 4 shows the quasi-steady RoS against wind speed over horizontal terrain obtained using FDS and three empirical models: the CSIRO [7], the McArthur mark V [35], and the 20% rule of thumb [10] models. All predictions are under fully cured conditions. The CSIRO model includes three different equations for estimating the RoS, namely Eq. (12) for natural grass conditions, Eq. (13) for grass cut or grazed, and Eq. (14) for grass heavily cut or eaten out.

$$RoS = \begin{cases} \left(0.054 + 0.269\, u_{10}\right) \phi_M\, \phi_C & \text{if } u_{10} \le 5 \text{ km/h} \\ \left(1.4 + 0.838\, (u_{10} - 5)^{0.844}\right) \phi_M\, \phi_C & \text{if } u_{10} > 5 \text{ km/h} \end{cases} \quad (12)$$

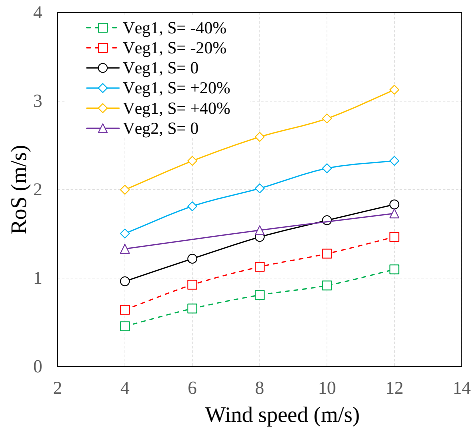

(a) $H_g = 0.2$ m.

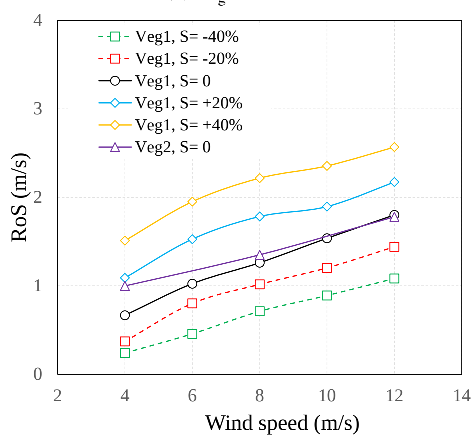

(b) $H_g = 0.5$ m.

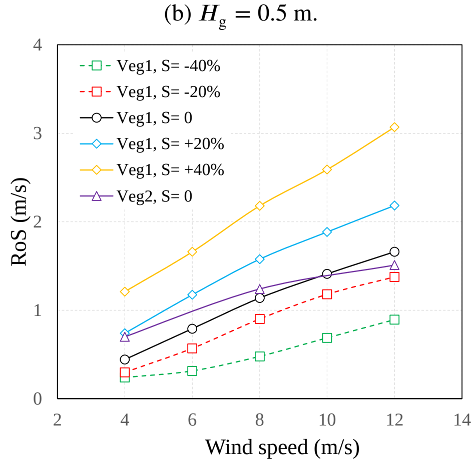

(c) $H_g = 1$ m.

Figure 3: Quasi-steady RoS at different wind speeds and slopes.

$$RoS = \begin{cases} \left(0.054 + 0.209\, u_{10}\right) \phi_M\, \phi_C & \text{if } u_{10} \leq 5 \text{ km/h} \\ \left(1.1 + 0.715\, (u_{10} - 5)^{0.844}\right) \phi_M\, \phi_C & \text{if } u_{10} > 5 \text{ km/h} \end{cases} \quad (13)$$

$$RoS = \left(0.55 + 0.357\, (u_{10} - 5)^{0.844}\right) \phi_M\, \phi_C \text{ if } u_{10} > 5 \text{ km/h} \quad (14)$$

where ϕ_M is the fuel moisture coefficient [7] and ϕ_C is the curing coefficient [11] calculated as follows:

$$\phi_M = \begin{cases} e^{-0.108\, M} & \text{if } M \leq 12\ \% \\ 0.684 - 0.0342\, M & \text{if } M \geq 12\ \% \text{ and } u_{10} < 10 \text{ km/h} \\ 0.547 - 0.0228\, M & \text{if } M \geq 12\ \% \text{ and } u_{10} \geq 10 \text{ km/h} \end{cases} \quad (15)$$

$$\phi_C = \frac{1.12}{1 + 103.99\, e^{-0.0996\, (C-20)}} \quad (16)$$

where C represents the degree of grass curing.

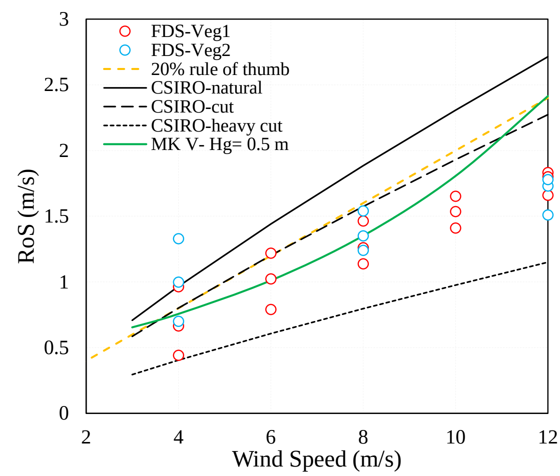

Figure 4: Quasy-steady RoS against wind speed over horizontal terrain obtained using FDS, CSIRO model, McArthur V model, and 20 % rule of thumb.

The RoS in McArthur mark V model is directly related to the grassland fire danger index (GFDI) as follows:

$$RoS = 0.13 \text{ GFDI} \quad (17)$$

where GFDI is as in Eq. (18) for $M < 18.8$ %:

$$\text{GFDI} = 3.35\, W\, e^{-0.0897\, M + 0.0403\, u_{10}}. \quad (18)$$

Since McArthur's model includes the effect of the fuel load, the equivalent fuel load for Veg_1 with $H_g = 50$ cm is utilised to calculate the corresponding RoS.

As expected, Fig. 4 shows that all models predict the RoS to increase with the wind speed, although the predicted values differ. These differences become larger for increasing wind speeds, with the FDS simulations clearly underestimating the empirical models' predictions. Notably, the CSIRO and the 20 % rule of thumb models show linear trends, while the influence of increasing wind speed on the RoS increases for the McArthur mark V model and decreases for FDS.

3.2. RoS as a function of terrain slope

As described in Section 2.6, the effect of bulk density on fire behaviour is studied solely on horizontal terrain. Therefore, this section focuses on the first fuel type (Veg_1).

Fig. 5a shows the quasi-steady RoS against terrain slope obtained by FDS for three vegetation heights and two wind speeds. Unsurprisingly, the RoS is higher for the higher wind speed, and increases monotonically with increasing slopes. Negative and positive slopes mean downhill and uphill propagation, respectively. As before, the RoS is higher for shorter grasses, which is more evident for $u_{10} = 6$ m/s. This trend seemingly diminishes as wind speed increases. For $u_{10} = 12$ m/s and small slopes, the influence of the grass height on the RoS is minimal.

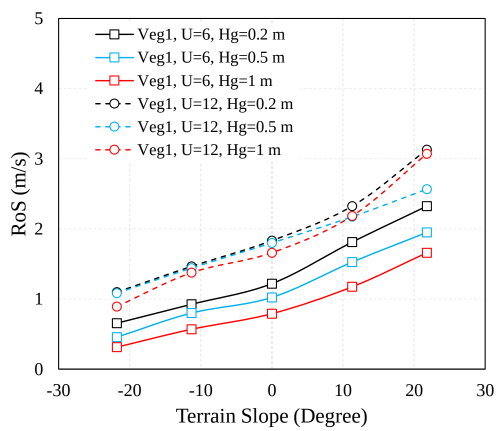

(a) RoS vs terrain slope

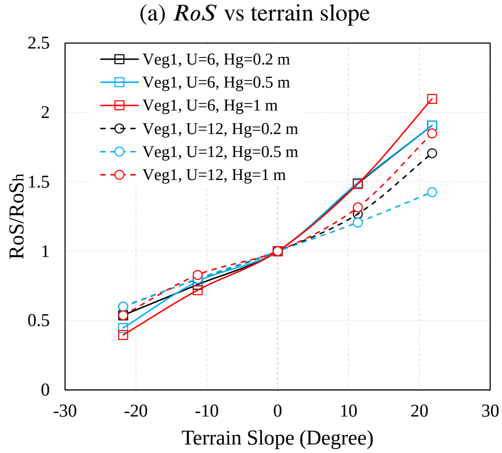

(b) RoS/RoS_h vs terrain slope

Figure 5: RoS and RoS/RoS_h ratio against terrain slopes for two wind speeds and three vegetation heights.

Fig. 5b presents the ratio of the RoS at each terrain slope to the corresponding RoS over horizontal terrain (RoS/RoS_h) for two wind speeds and three vegetation heights. An increase in the slope of the lines when S>|11.8°| indicates that the influence of the terrain slope on the RoS/RoS_h ratio is more pronounced for larger magnitudes of the slope (whether uphill or downhill). Besides, it could be observed that the effect of the terrain slope on the RoS/RoS_h ratio is more pronounced at lower wind speeds: it increases faster uphill and decreases faster downhill.Under such conditions, fire propagation is primarily influenced by buoyancy forces, which leads to a plume-dominated propagation. This effect tends to diminish at higher wind speeds, as the fire propagation is then driven by the wind. Additionally, it can be concluded that the influence of terrain slope on accelerating the RoS on steeper terrain relative to the RoS on horizontal terrain (RoS/RoS_h) is more significant in cases with tall vegetation ($H_\mathrm{g} = 1$ m), signifying the combined effect of vegetation and terrain slope on free propagation dynamics.

Fig. 6 shows the quasi-steady RoS against terrain slope obtained from FDS simulations (red markers) for vegetation height $H_\mathrm{g} = 0.2$ m, and wind speeds $u_{10} = 6$ m/s and $u_{10} = 12$ m/s . These estimations are compared against those obtained from simulations in [21], and from the CSIRO [7] and the McArthur mark V [35] empirical models. The latter is corrected for slope effect using the correction factors in [35] as adopted in [21] and shown below:

$$RoS = RoS_\mathrm{h}\, e^{0.069S} \tag{19}$$

where RoS is the forward RoS in km/h, and S is the slope of the terrain in degrees.

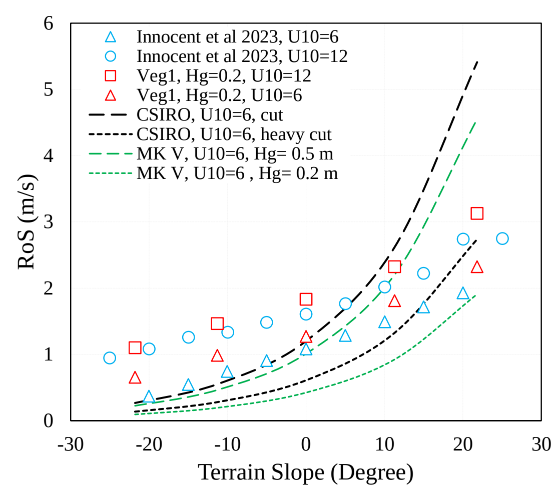

Figure 6: RoS against terrain slope obtained from simulations and from empirical models.

The RoS values obtained from the FDS simulations are loosely in agreement with those obtained from the simulations in [21]. The differences observed may be attributed to differences in the use of fuel models, wind models, grid size, and the longer ignition lines used in our study. While Innocent et al. [21] employed the FDS-BFM and a two-step thermal degradation model which neglects the exothermic char oxidation, our study uses the FDS-LPM and a three-step reaction model. Among the empirical models, the CSIRO-cut is the one showing some agreement with the simulations, especially for small magnitudes of the slope $S \in (-10, 10)$, although the rate of change of the RoS with respect to the terrain slope is steeper.

3.3. RoS as a function of vegetation characteristics

In previous sections, we examined the combined effects of wind speed, terrain slope, and vegetation height on the RoS of the fire. Simulation results indicated that, generally,

Table 4
Average and range of measured environmental and fire variables in [12] and [14].

Ref.	Vegetation		T (°C)	RH (%)	u_{10} (m/s)	W (kg.m^{-2})	H_g (m)	ρ_b (kg.m^{-3})	M (%)	RoS (m/s)	RoS/U_{10}	I (KW.m^{-1})
[12]	Wheat	mean	30.2	21.6	8.0	0.42	0.37	1.6	7.5	1.5	0.19	12131
		[range]	[24.8-38]	[13.6-31.7]	[5.2-10.8]	[0.32 -0.53]	[0.08-0.83]	[0.73-4.04]	[5.4-11.6]	[0.7-2.8]	[0.08-0.38]	[3858-27987]
[14]	Grass	mean	25.7	27.8	5.3	0.49	0.39	1.38	7.96	1.0	0.18	7868
		[range]	[16-33]	[6-59]	[2-13]	[0.17-1.05]	[0.16-0.93]	[0.43-3.0]	[3.5-12.6]	[0.2-2.5]	[0.1-0.3]	[1260-18703]

higher vegetation leads to lower RoS for constant bulk density (ρ_b). This is in agreement with [28]. However, in some cases under high wind speeds and steep upslope conditions, the RoS is higher in taller grasses.

The practice of mowing grasses is widely adopted as a management strategy to control and slow down the wildfire spread in grasslands around the world, particularly favoured by the Australian fire authorities. The rationale is that cutting the grass would result in a less intense and slower propagating fire [13]. This is supported by the experimental burns reported in [6] and [12]. In contrast, some studies such as [14] and [28] suggest that the RoS decreases with increasing vegetation height, and therefore the current practice of mowing grasses should be reconsidered. In this section, we address this question by analysing the RoS estimated from experiments and simulations under varying wind speeds and over flat terrain. The aim is to explore how vegetation height and bulk density affect the RoS of the fire.

Two studies are selected with seemingly contradictory results regarding the relationship between fuel height (H_g) and RoS of fire: grassland fire experiments in [14], and wheatland fire experiments in [12]. The aim is to investigate the sources of the contradictory results reported. The environmental and fuel conditions for both studies are summarised in Table 4. They are both performed in Australian territories under comparable temperature (T), relative humidity (RH), vegetation height (H_g), and moisture content (M) conditions. It is important to note that the bulk density reported in [12] refers specifically to the standing fuel, while the burning experiments are carried out in the presence of matted fuel on the ground. However, for fire intensity calculations, the total fuel load includes 80 % of matted fuel load as well. Consequently, we calculate bulk density as the consumed fuel divided by the fuel height. While both the standing fuel bulk density and this calculated bulk density yield similar trends and insights, we opted to use the latter for better visualisation and to maintain consistency with other calculations such as fire intensity and with [14].

The average RoS and intensity (I) from wheatland experiments in [12] ($RoS_{avg} = 1.5$ m/s) are higher than those from grassland experiments in [14] ($RoS_{avg} = 1$ m/s), which are seemingly due to the higher average wind speed during the wheatland experiments. However, experiments diverge primarily in their findings concerning the correlation between RoS and H_g. In the wheatland experiments, they are positively correlated (in agreement with the conclusions made by Cheney et al. [6]). In contrast, the grassland experiments report a negative correlation. To reconcile these conflicting outcomes, Cruz et al. [13] state that the positive correlation between RoS and H_g is sufficiently confirmed experimentally. They attributed the grassland study's contradictory conclusion to structural differences in the grasslands, which likely obscured the effect of H_g and led to misleading conclusions. Instead, Sutherland et al. [43] suggested that the differences are mainly due to different propagation modes: while the wheatland experiments primarily represented wind-driven fires, the grassland experiments were predominantly buoyancy-driven. They concluded that higher H_g leads to higher RoS. Fig. 7 shows experimental data from [14] and [12] alongside data obtained from our FDS simulations. Properties studied includes fire RoS, H_g, bulk density (ρ_b), and fuel load (W).

Fig. 7a shows the relationship between RoS and H_g, including experimental data from [14] and [12] alongside results from FDS simulations carried out in this study. The positive correlation in [12] contrasts with the negative correlation in [14] and from our FDS simulations. A linear fit is applied for visualisation purposes only, acknowledging that it might not be appropriate for all datasets. Notably, the use of the RoS may be misleading, as it is influenced by the ambient wind speed. Hence, using the RoS/u_{10} ratio provides a more reliable representation of the data, as depicted in Fig. 7b. A strong positive correlation between RoS/u_{10} and H_g for the wheatlands experiments is evident, while the significant negative correlation in grassland experiments and our simulations no longer appears. This suggests that there is no (RoS/u_{10})–H_g correlation for grassland experiments in [14] and our FDS simulations. A similar behaviour is observed for (RoS/u_{10})–W in Fig. 7c, suggesting that neither H_g nor W can sufficiently characterise the fire behaviour. However, when plotting the non-dimensional RoS/u_{10} ratio against ρ_b, a clear negative correlation emerges across all datasets, as shown in Fig. 7d. It is consistent with the findings in [5] that increasing ρ_b leads to decreasing RoS for no-wind conditions. Here, however, this is still valid in the presence of wind. Accounting for fuel moisture (M), Fig. 7e shows $RoS/u_{10}/M$ against ρ_b, where a negative correlation can be observed, better trend agreement, and Pearson correlation coefficients $R_p = -0.57$ for wheatland fire and $R_p = -0.42$ for grassland fire datasets. The most intriguing behaviour is found when plotting $RoS/u_{10}/M$ against H_g in Fig. 7f. For both experimental datasets, a positive trend is found with a Pearson correlation coefficient $R_p = 0.59$ for [12] and $R_p = 0.19$ for [14]. This highlights a consistent relationship between RoS and H_g when corrected for wind speed and moisture, reconciling the seemingly contradicting findings in [12] and [14].

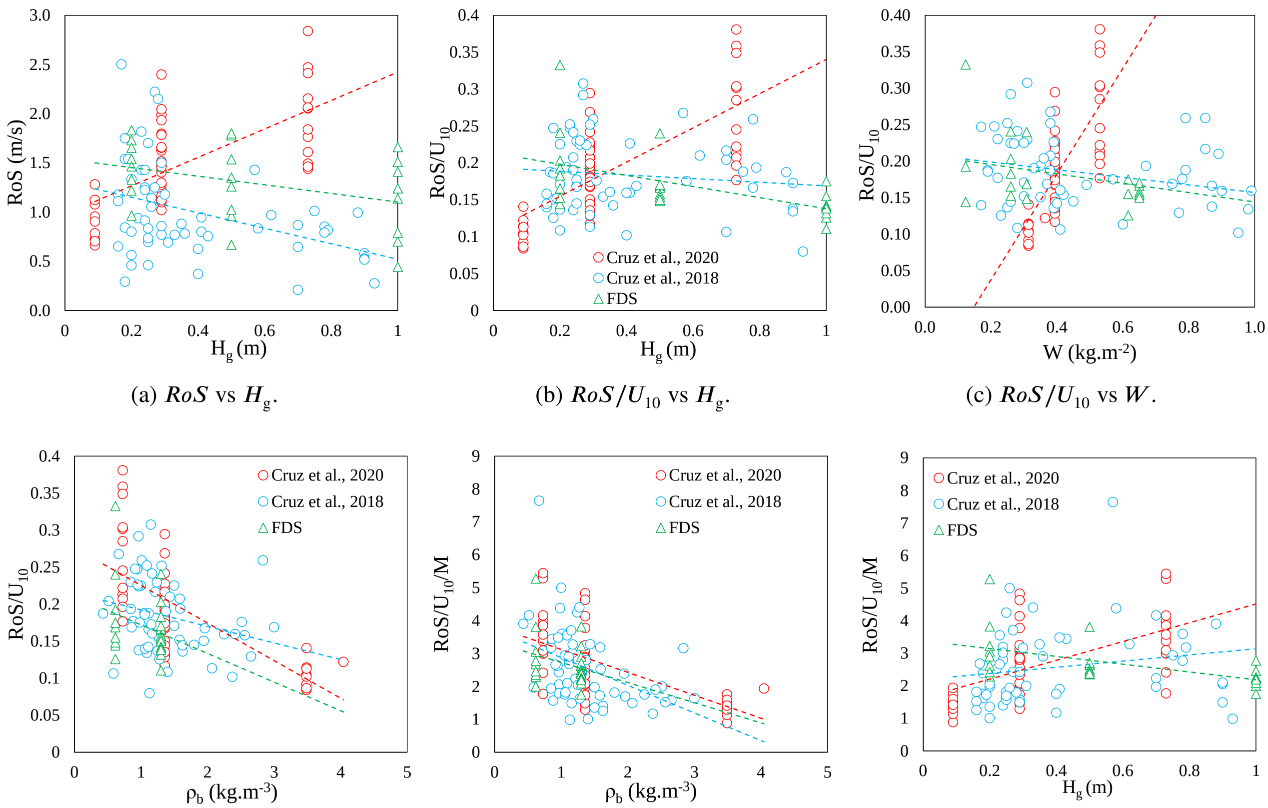

(a) RoS vs H_g. (b) RoS/U_{10} vs H_g. (c) RoS/U_{10} vs W.

(d) RoS/U_{10} vs ρ_b. (e) $RoS/U_{10}/M$ vs ρ_b. (f) $RoS/U_{10}/M$ vs H_g.

Figure 7: Distribution and trend of data including fire RoS, fuel height (H_g), fuel load (W), fuel moisture (M), bulk density (ρ_b), and wind speed 10 m AGL (u_{10}) for grassland experiments [14] (2018, blue markers), wheatland experiments [12] (2020, red markers), and our FDS simulations (2024, green markers).

To summarise, the RoS/u_{10} ratio increases with vegetation height (H_g) for constant moisture (M). Nevertheless, the slopes of the trends in both datasets exhibit distinct magnitudes, reflecting the effect of various parameters that affect fire behaviour, such as atmospheric humidity and temperature, and the surface-area-to-volume ratio of the fuel. However, contrary to experimental results, our FDS simulations indicate a weak negative correlation which initially appears counter-intuitive. Section 4.1 delves into the potential reasons behind this discrepancy, and demonstrates that FDS is able to accurately reproduce the correct relationship between $RoS/u_{10}/M$ and H_g.

3.4. RoS as a function of propagation mode

Despite the diverse range of burning conditions, fuel types, vegetation heights, terrain conditions, and other atmospheric parameters like moisture, a unifying perspective can be achieved by examining their collective impact on fire intensity (I), and consequently, on the equilibrium of buoyancy and inertial forces within the fire front [31]. Therefore, Fig. 8 presents the RoS/u_{10} ratio against N_c (Byram number) for all datasets used in this study, along with a power law fit across the datasets. For wind-driven fires, particularly for $N_c < 1$, a saturation of data points is observed in the range $RoS/u_{10} \in (0.08, 0.20)$ for all datasets, converging towards a state independent of N_c. This agrees with Morvan et al. [31], who suggested that fire propagation in this state is solely a function of M. However, a broad range of RoS/u_{10} values can be observed for larger values of N_c, increasing as N_c increases.

4. Discussion

The previous section provided insight into the simulation results and the reanalysis of experimental datasets. However, questions were raised or remained partially unanswered, as they require the consideration of additional factors that affect the fire, including the fire propagation mode. Consequently, this section aims to combine analysis conclusions and fire propagation modes to address two key questions:

1. Is FDS capable of accurately reproducing the effect of grass height on wildfire propagation as observed in experimental field studies?

2. Does cutting grass effectively slow down the propagation of wildfires?

4.1. Are FDS results counter-intuitive?

The previous section revealed that FDS simulations describe a negative correlation between $RoS/u_{10}/M$ and H_g.

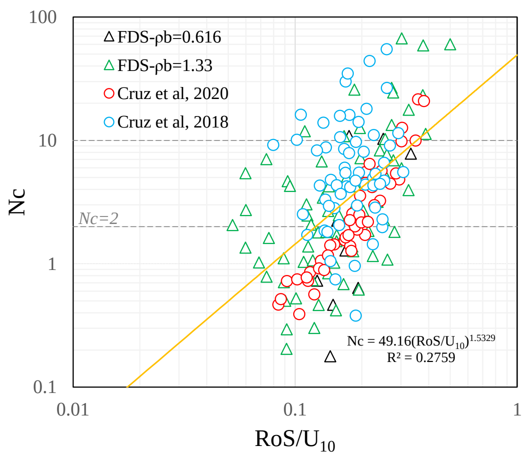

Figure 8: RoS/u_{10} ratio against the Byram number (N_C) for the combined dataset of simulations and experimental results. Dashed lines show $N_C = 2$ and $N_C = 10$, where the fire propagation regime is wind-driven for $N_C < 2$ and plume-dominated for $N_C > 10$. The solid orange line represents the best linear fit for the whole dataset.

Similarly, Sutherland et al. [43, 28] reported a negative correlation between RoS and H_g, whereas experimental data found a positive correlation instead. However, it is crucial to highlight that all simulations in [43, 28] and the majority of our simulations assume constant bulk density (ρ_b) across all H_g. In contrast, natural vegetation in the experimental datasets shows decreasing ρ_b for increasing H_g. The Pearson correlation coefficient between H_g and ρ_b was found to be $R_p = -0.62$ in [12] and $R_p = -0.37$ in [14]. Cruz et al. [13] argues that changing H_g while keeping ρ_b constant—as in [43, 28] and in our simulations—solely changes the amount of fuel available for combustion, and that this does not suffice to explain the effect of these two fuel characteristics on the RoS. Besides, the representation of fuel as a homogeneous rigid layer that does not bend with the wind might have contributed to an incorrect estimation of drag coefficient and roughness length.

While we acknowledge the potential effect of vegetation representation and flexibility on the exerted drag and RoS, our analyses suggest that the disparity in ρ_b between simulated and natural vegetation significantly contributes to the observed differences in $RoS/u_{10}/M$ and H_g correlations between FDS simulations and experimental observations. To further examine the effect of ρ_b on RoS and on the mode of propagation of the fire, Figs. 9a to 9c show the FDS predictions of how RoS and H_g are related at three wind speeds (u_{10}), three terrain slopes (S), and two ρ_b. The corresponding values of the Byram convective number (N_c) for each of these cases are shown in Figs. 9d to 9f.

As previously mentioned, higher H_g with constant ρ_b leads to a reduction in the RoS, irrespective of the terrain slope or fire propagation mode. The only exception occurs for Veg_1, $S = 40\,\%$, and $u_{10} = 12\,\text{m/s}$, in which case higher H_g between 0.5 m and 1 m results in higher RoS. This might be influenced by the shift in the fire propagation regime, as characterised by N_c (red line) crossing the $N_c = 2$ threshold at $H_g \approx 0.5$ m in Fig. 9f.

Thus, our findings are not in agreement with those in [43], which state that RoS increases with increasing H_g for constant ρ_b and wind-driven fires. However, it is important to note that their results are drawn from experiments with constant ρ_b and $H_g < 0.2$ m, which is below the range considered in our simulations. Furthermore, the results obtained in our study using a wide range of wind speeds and terrain slopes do not confirm their observations, suggesting that factors beyond the fire propagation mode might have influenced the outcomes of their research.

Considering the effect of ρ_b on RoS and N_C, it can be observed in Figs. 9b and 9e that RoS for Veg_1 (higher ρ_b) is smaller than that of Veg_2 (lower ρ_b) for $N_c \gg 2$ (plume-dominated and transitory regimes). This observation aligns with the conclusion in Section 3.3 that an increase in ρ_b leads to a reduction in RoS. Notably, this discrepancy tends to diminish as $N_c \to 2$ (blue lines in Figs. 9b and 9e). However, for N_c well below the threshold of two (red lines, wind-driven fires), an interesting trend emerges: RoS for Veg_1 ($\rho_b = 1.33$ kg/m^3) is slightly higher than that for Veg_2 ($\rho_b = 0.616$ kg/m^3). This highlights a distinctive trend in wind-driven fires, which deviates from the general pattern observed in plume-dominated fires.

Fig. 10 depicts the RoS/u_{10} and corresponding N_c as a function of H_g, imitating the lower ρ_b characteristic seen in taller natural vegetation. For each case, the RoS/u_{10} of shorter grass is extracted from Veg_1 with $\rho_b = 1.33$ kg/m^3, while that of taller grass is extracted from Veg_2 with $\rho_b = 0.616$ kg/m^3. Consequently, for the solid black line, RoS at H_g=0.2 m comes from Veg_1 and RoS at H_g=0.5 m corresponds to Veg_2 with lower bulk density.

It is observed that for transitory and plume-dominated propagation modes ($N_c > 2$), the RoS/u_{10} ratio increases with increasing H_g (simultaneously decreasing ρ_b). However, for wind-driven fires ($N_c < 2$), the RoS/u_{10} ratio decreases with increasing H_g (and simultaneously decreasing ρ_b). This latter behaviour was not observed in the wheatland experiments in [12], possibly due to the complexity and variability of experimental conditions and scattered data points, underscoring the need for further controlled experiments for wind-driven conditions.

In summary, it has been demonstrated that FDS can realistically model the relationship between the RoS/u_{10} ratio and vegetation height (H_g). This holds true provided that bulk density (ρ_b) decreases as H_g increases, which is a characteristic observed in natural vegetation types.

4.2. To cut or not to cut?

Mowing grasses is a widely accepted practice to curb the RoS of wildfires. While reducing H_g can indeed decrease fire intensity and therefore make the fire more manageable, it also makes it more prone to becoming wind-driven. Besides, our analyses suggest that the bulk density of the vegetation layer decreases ($\rho_b \downarrow$) as the vegetation grows taller ($H_g \uparrow$).

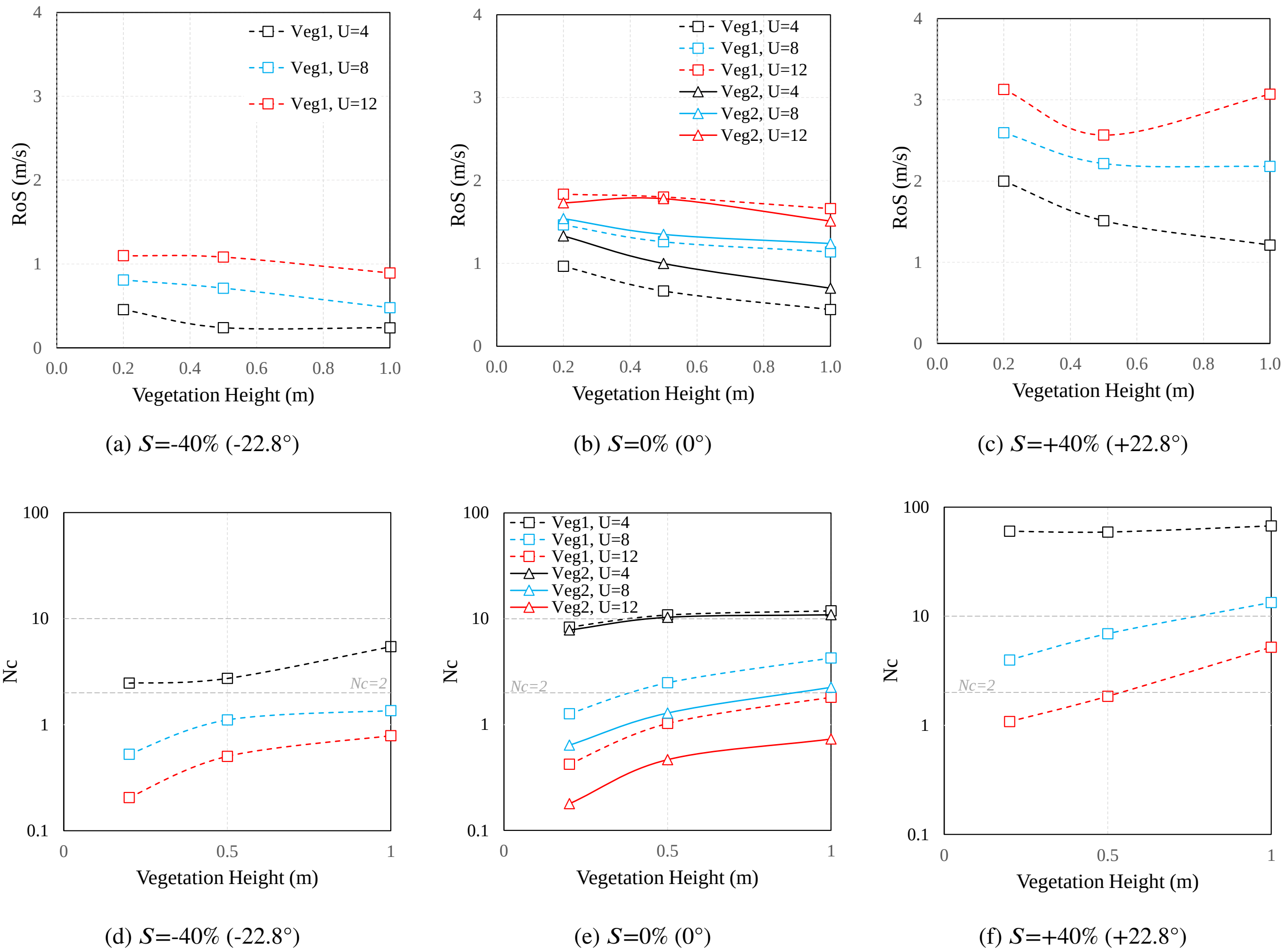

(a) S=-40% (-22.8°) (b) S=0% (0°) (c) S=+40% (+22.8°)

(d) S=-40% (-22.8°) (e) S=0% (0°) (f) S=+40% (+22.8°)

Figure 9: RoS (a)–(c) and the corresponding Byram convective number (N_c) (d)–(f) against vegetation height (H_g) for two different vegetations, Veg_1 and Veg_2, with respective bulk densities of ρ_b = 1.313 kg/m^3 and ρ_b = 0.616 kg/m^3, at three wind speeds (u_{10}) and three terrain slopes (S). The N_C = 2 and N_C = 10 thresholds separate two fire propagation regimes, namely wind-driven ($N_C < 2$) and plume-dominated ($N_C > 10$).

From the analyses in previous sections, it can be stated that increasing bulk density (ρ_b ↑) reduces the rate of spread (RoS/u_{10} ↓). Hence, RoS/u_{10} decreases with shorter grass (H_g ↓). Therefore, mowing grasses may be an effective wildfire management strategy, as long as ρ_b increases as H_g decreases. However, it is important to note that this is valid for constant moisture (M). Higher values of M may overshadow the effect of H_g.

The probability of wind-driven fire also increases when cutting the grass due to reduced fire intensity. Our simulations indicate that increasing bulk density (ρ_b ↑) may lead to faster propagation (RoS/u_{10} ↑) for wind-driven fires ($N_c < 2$), though this behaviour was not observed in the wheatland experiments in [12]. Moreover, simulations in [43] suggest that taller vegetation may promote higher RoS for wind-driven fires, even if ρ_b is constant. Further experimental research is required to accurately determine if this effect can outweigh the benefits of reduced vegetation height.

5. Conclusions

The likelihood and intensity of wildfires have increased around the world due to global climate changes. Although grasslands cover less than 40 % of the Earth's surface, they encompass the majority of the burned area worldwide. This highlights the need for management strategies to confine the spread of wildfires in grasslands. One of these strategies is to cut or graze the grasses to limit the fire spread and intensity. However, this strategy has been challenged during the past few years based on results from a series of field experiments and numerical simulations.

This study combined contradicting field experiments with an extensive set of three-dimensional field-scale simulations to study the effect of vegetation height and vegetation bulk density on wildfire propagation dynamics under different atmospheric and terrain conditions. Results indicate that increasing terrain slope (uphill conditions) or wind speed leads to an increased rate of spread, irrespective of the vegetation height and bulk density. Moreover, this study underscores the importance of bulk density in fire dynamics,

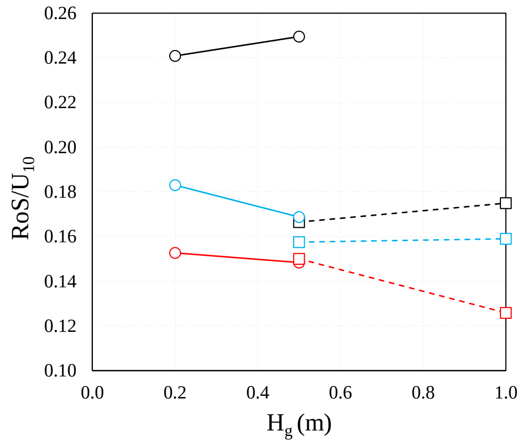

(a) RoS/u_{10} ratio against H_g.

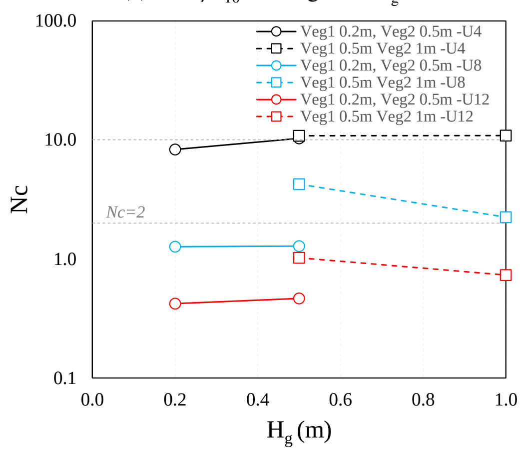

(b) Corresponding Nc against H_g.

Figure 10: RoS/u_{10} ratio and the corresponding Byram convective number (N_c) against vegetation height (H_g) for three wind speeds. For each line, the first point is extracted from Veg_1 with $\rho_b = 1.33$ kg/m^3 and the second point from Veg_2 with $\rho_b = 0.616$ kg/m^3.

with findings revealing that the fire rate of spread decreases with increasing vegetation bulk density, provided that the fire is plume-dominated.

It was found that the bulk density of natural vegetation—at least those considered in this study—decreases as the vegetation grows taller. Thus, the relationship between vegetation height and fire RoS seems to be inherently linked to the variation in vegetation bulk density. Simulation results suggest that increasing the vegetation height, while maintaining bulk density constant, leads to a reduced RoS. Conversely, in natural vegetation, where the bulk density decreases with increasing height, the RoS increases for taller vegetation. This implies that reduced bulk density is a primary driver, as opposed to vegetation height alone. However, it must be noted that, even though the above-mentioned behaviours were observed in experimental data of both plume-dominated and wind-driven propagation modes, further simulations suggested potential reversals under wind-driven fire conditions. The lack of experimental data to validate the extreme behaviours observed in simulations emphasises the importance of designing and performing more field tests to support the investigation of fire dynamics. Such experimental studies are crucial for refining existing and projected grassland fire management strategies, especially for regions prone to high wind conditions.

CRediT authorship contribution statement

Mohammad Tavakol Sadrabadi: Conceptualization, Methodology, Software, Writing, Investigation, Visualization. **Mauro Sebastián Innocente:** Conceptualization, Methodology, Software, Writing, Supervision, Resources, Visualization.

References

[1] Albini, F. A. (1976). Estimating wildfire behavior and effects. Technical Report INT-GTR-30, U.S. Department of Agriculture, Forest Service, Intermountain Forest and Range Experiment Station, Ogden, UT.

[2] B. Porterie, J. L. Consalvi, A. K. and Loraud, J. C. (2005). Predicting wildland fire behavior and emissions using a fine-scale physical model. *Numerical Heat Transfer, Part A: Applications*, 47(6):571–591.

[3] Boardman, C. R., Dietenberger, M. A., and Weise, D. R. (2021). Specific heat capacity of wildland foliar fuels to 434 °c. *Fuel*, 292:120396.

[4] Boonmee, N. and Quintiere, J. (2005). Glowing ignition of wood: the onset of surface combustion. *Proceedings of the Combustion Institute*, 30(2):2303–2310.

[5] Campbell-Lochrie, Z., Walker-Ravena, C., Gallagher, M., Skowronski, N., Mueller, E. V., and Hadden, R. M. (2021). Investigation of the role of bulk properties and in-bed structure in the flow regime of buoyancy-dominated flame spread in porous fuel beds. *Fire Safety Journal*, 120:103035. Fire Safety Science: Proceedings of the 13th International Symposium.

[6] Cheney, N., Gould, J., and Catchpole, W. (1993). The influence of fuel, weather and fire shape variables on fire-spread in grasslands. *International Journal of Wildland Fire*, 3(1):31–44.

[7] Cheney, N. P., Gould, J. S., and Catchpole, W. R. (1998). Prediction of fire spread in grasslands. *International Journal of Wildland Fire*, 8:1–13.

[8] Cruz, M. G. and Alexander, M. E. (2019). The 10% wind speed rule of thumb for estimating a wildfire's forward rate of spread in forests and shrublands. *Annals of Forest Science*, 76:44.

[9] Cruz, M. G., Alexander, M. E., and Kilinc, M. (2022a). Wildfire rates of spread in grasslands under critical burning conditions. *Fire*, 5(2).

[10] Cruz, M. G., Alexander, M. E., and Kilinc, M. (2022b). Wildfire rates of spread in grasslands under critical burning conditions. *Fire*, 5(2).

[11] Cruz, M. G., Gould, J. S., Kidnie, S., Bessell, R., Nichols, D., and Slijepcevic, A. (2015). Effects of curing on grassfires: Ii. effect of grass senescence on the rate of fire spread. *International Journal of Wildland Fire*, 24:838–848.

[12] Cruz, M. G., Hurley, R. J., Bessell, R., and Sullivan, A. L. (2020). Fire behaviour in wheat crops – effect of fuel structure on rate of fire spread. *International Journal of Wildland Fire*, 29:258–271.

[13] Cruz, M. G., Sullivan, A. L., and Gould, J. S. (2021). The effect of fuel bed height in grass fire spread: addressing the findings and recommendations of moinuddin et al. (2018). *International Journal of Wildland Fire*, 30:215–220.

[14] Cruz, M. G., Sullivan, A. L., Gould, J. S., Hurley, R. J., and Plucinski, M. P. (2018). Got to burn to learn: the effect of fuel load on grassland fire behaviour and its management implications. *International Journal of Wildland Fire*, 27:727–741.

[15] Finney, M. A. (1998). Farsite: Fire area simulator-model development and evaluation. Technical report.

[16] for National Statistics, O. (2015). Uk natural capital: Land cover in the uk.

[17] Grasso, P. and Innocente, M. S. (2018). A two-dimensional reaction-advection- diffusion model of the spread of fire in wildlands. In *Advances in Forest Fire Research*.

[18] Grasso, P. and Innocente, M. S. (2020). Physics-based model of wildfire propagation towards faster-than-real-time simulations. *Computers & Mathematics with Applications*, 80(5):790–808.

[19] Grishin, A. (1997). *Mathematical Modeling of Forest Fires and New Methods of Fighting Them*. Publishing House of the Tomsk State University.

[20] Guo, H., Xiang, D., Kong, L., Gao, Y., and Zhang, Y. (2023). Upslope fire spread and heat transfer mechanism over a pine needle fuel bed with different slopes and winds. *Applied Thermal Engineering*, 229:120605.

[21] Innocent, J., Sutherland, D., Khan, N., and Moinuddin, K. (2023). Physics-based simulations of grassfire propagation on sloped terrain at field scale: motivations, model reliability, rate of spread and fire intensity. *International Journal of Wildland Fire*, 32:496–512.

[22] Jarrin, N., Uribe, J.-C., Prosser, R., and Laurence, D. (2008). *Synthetic inflow boundary conditions for wall bounded flows*, volume 97 of *Notes on Numerical Fluid Mechanics and Multidisciplinary Design*. Springer Nature, United States.

[23] Leys, B. A., Marlon, J. R., Umbanhowar, C., and Vannière, B. (2018). Global fire history of grassland biomes. *Ecology and Evolution*, 8(17):8831–8852.

[24] McArthur, A. G. (1969). The tasmanian bushfires of 7th february 1967 and associated fire behaviour characteristics. In operation Programme, T. T. C., editor, *Mass Fire Symposium: The Technical Cooperation Programme*, volume 1, page Paper A7, Canberra, ACT. Defence Standards Laboratories.

[25] McGrattan, K., Hostikka, S., Floyd, J., McDermott, R., Vanella, M., and Mueller, E. (2023). *Fire Dynamics Simulator User's Guide*, sixth edition.

[26] Mell, W., Jenkins, M. A., Gould, J., and Cheney, P. (2007). A physics-based approach to modelling grassland fires. *International Journal of Wildland Fire*, 16(1):1.

[27] Moinuddin, K., Khan, N., and Sutherland, D. (2021). Numerical study on effect of relative humidity (and fuel moisture) on modes of grassfire propagation. *Fire Safety Journal*, 125:103422.

[28] Moinuddin, K. A. M., Sutherland, D., and Mell, W. (2018). Simulation study of grass fire using a physics-based model: striving towards numerical rigour and the effect of grass height on the rate of spread. *International Journal of Wildland Fire*, 27(12):800–814.

[29] Morandini, F., Silvani, X., luc Dupuy, J., and Susset, A. (2018). Fire spread across a sloping fuel bed: Flame dynamics and heat transfers. *Combustion and Flame*, 190:158–170.

[30] Morvan, D. (2014). Wind effects, unsteady behaviors, and regimes of propagation of surface fires in open field. *Combustion Science and Technology*, 186(7):869–888.

[31] Morvan, D. and Frangieh, N. (2018). Wildland fires behaviour: wind effect versus byram's convective number and consequences upon the regime of propagation. *International Journal of Wildland Fire*, 27:636–641.

[32] Mueller, E. V., Campbell-Lochrie, Z., Walker-Ravena, C., and Hadden, R. M. (2023). Numerical simulations of flame spread in pine needle beds using simple thermal decomposition models. *Fire Safety Journal*, 141:103886.

[33] Mueller, E. V., Skowronski, N. S., Clark, K. L., Gallagher, M. R., Mell, W. E., Simeoni, A., and Hadden, R. M. (2021). Detailed physical modeling of wildland fire dynamics at field scale - an experimentally informed evaluation. *Fire Safety Journal*, 120:103051. Fire Safety Science: Proceedings of the 13th International Symposium.

[34] Nelson, R. M. (2015). Re-analysis of wind and slope effects on flame characteristics of mediterranean shrub fires. *International Journal of Wildland Fire*, 24:1001–1007.

[35] NOBLE, I. R., GILL, A. M., and BARY, G. A. V. (1980). Mcarthur's fire-danger meters expressed as equations. *Australian Journal of Ecology*, 5(2):201–203.

[36] (NWCG), N. W. C. G. Atmospheric stability.

[37] O'Mara, F. P. (2012). The role of grasslands in food security and climate change. *Annals of Botany*, 110(6):1263–1270.

[38] Petersen, E. L., Mortensen, N. G., Landberg, L., Højstrup, J., and Frank, H. P. (1998). Wind power meteorology. part i: climate and turbulence. *Wind Energy*, 1(S1):25–45.

[39] Pimont, F., Dupuy, J.-L., and Linn, R. R. (2012). Coupled slope and wind effects on fire spread with influences of fire size: a numerical study using firetec. *International Journal of Wildland Fire*, 21:828–842.

[40] Potter, B. E. (2012). Atmospheric interactions with wildland fire behaviour–i. basic surface interactions, vertical profiles and synoptic structures. *International Journal of Wildland Fire*, 21:779–801.

[41] Rothermel, R. C. (1972). A mathematical model for predicting fire spread in wildland fuels. Research paper, Rocky Mountain Research Station, Ogden, UT.

[42] Sjöström, J. and Granström, A. (2023). A phenology-driven fire danger index for northern grasslands. *International Journal of Wildland Fire*, 32:1332–1346.

[43] Sutherland, D., Sharples, J. J., Mell, W., and Moinuddin, K. A. M. (2021). A response to comments of cruz et al. on: 'simulation study of grass fire using a physics-based model: striving towards numerical rigour and the effect of grass height on the rate of spread'. *International Journal of Wildland Fire*, 30:221–223.

[44] Sánchez-Monroy, X., Mell, W., Torres-Arenas, J., and Butler, B. (2019). Fire spread upslope: Numerical simulation of laboratory experiments. *Fire Safety Journal*, 108:102844.

[45] United Nations Environment Programme (2022). Spreading like wildfire: The rising threat of extraordinary landscape fires. Technical report, United Nations Environment Programme.

[46] Vanella, M., McGrattan, K., McDermott, R., Forney, G., Mell, W., Gissi, E., and Fiorucci, P. (2021). A multi-fidelity framework for wildland fire behavior simulations over complex terrain. *Atmosphere*, 12(2).

[47] Weise, D. R. and Biging, G. S. (1994). Effects of wind velocity and slope on fire behavior. In Kashiwagi, T., editor, *Fire Safety Science Proceedings of the Fourth International Symposium*, pages 1041–1051, Boston, MA. Intl. Assoc. for Fire Safety Science.

[48] Wu, Y., Xing, H., and Atkinson, G. (2000). Interaction of fire plume with inclined surface. *Fire Safety Journal*, 35(4):391–403.